Andean Geology 37 (2): 433-441. July, 2010

Andean Geology
formerly Revista Geológica de Chile
www.scielo.cl/andgeol.htm

Compositional variations revealed by ASTER image analysis of the Viedma Volcano, southern Andes Volcanic Zone

Chiaki Kobayashi[1], Yuji Orihashi[2], Daiji Hiarata[3], José A. Naranjo[4], Makoto Kobayashi[5], Ryo Anma[6]

[1] *Earth Remote Sensing Data Analysis Center, Chuo, Tokyo 104-0054, Japan.*
kobayashi@ersdac.or.jp
[2] *Earthquake Research Institute, the University of Tokyo, Bunkyo, Tokyo 113-0032, Japan.*
oripachi@eri.u-tokyo.ac.jp
[3] *Kanagawa Prefectural Museum of Natural History, Odawara, Kanagawa 250-0031, Japan.*
hirata@nh.kanagawa-museum.jp
[4] *Servicio Nacional de Geología y Minería, Av. Santa María 0104, Providencia, Santiago, Chile.*
jnaranjo@sernageomin.cl
[5] *Dia Consultants Company Limited, Saitama, Saitama 331-8638, Japan.*
m.kobayashi@diaconsult.co.jp
[6] *Graduate School of Life and Environmental Sciences, University of Tsukuba, Tsukuba, Ibaraki 305-8572, Japan.*
ranma@sakura.cc.tsukuba.ac.jp

ABSTRACT. We conducted a lithological mapping of the Viedma volcano, one of five volcanoes in the Andean Austral Volcanic Zone (AVZ), using remote sensing techniques. We used data of the Advanced Spaceborne Thermal Emission and Reflection radiometer (ASTER) sensor which is highly effective in geological research, to understand build-up processes and to deduce compositional variation of the Viedma volcano emerging from the South Patagonian ice field. The volcanic edifice was divided into bright parts that mainly compose the eastern flank of the volcano and dark parts at the central crater area based on the observation in visible and near infrared ranges. The SiO_2 concentration was calculated using the bands in the visible and thermal infrared regions. The dark part and the bright part have approximately 51 wt% and 63 wt% average SiO_2 content respectively, indicating that the exposures of the Viedma volcano have a wide variation in SiO_2 concentration. Although, according to other authors, ejecta from the Viedma volcano have 64-66 wt% SiO_2 and other AVZ volcanoes are essentially monolithologic dacite/andesite volcanoes, the edifice of the Viedma volcano appears to be composed mostly of basalts or older rocks/basement with low silica contents.

Keywords: ASTER, Viedma volcano, SiO_2 wt%, Andean Austral Volcanic Zone, Chile.

RESUMEN. Variaciones composicionales reveladas mediante análisis de imágenes ASTER del volcán Viedma, Zona Volcánica Andina Austral. Mediante el uso de técnica de sensoría remota se ha desarrollado un mapeo litológico del volcán Viedma, uno de los cinco volcanes de la Zona Volcánica Andina Austral (ZVA). Para este efecto, se ha utilizado el radiómetro 'Advanced Spaceborne Thermal Emission and Reflection' (ASTER) que es muy efectivo en investigación geológica, para entender los procesos que han controlado la estructura y deducir las variaciones composicionales del volcán Viedma, que sobresale levemente de la superficie del campo de hielo Patagónico Sur. Sobre la base de la observación en el intervalo del espectro visible e infrarrojo cercano, en el edificio se distinguen partes brillantes que corresponden al flanco oriental del volcán y partes oscuras en el área del cráter central. La concentración de SiO_2 se calculó a través del uso de las bandas en las regiones visibles e infrarrojo termal. Las partes oscura y brillante tienen un promedio aproximado de 51% y 63% de SiO_2 en peso, respectivamente, lo que indica que el volcán Viedma expone una amplia diferenciación de las concentraciones de SiO_2. Aunque, según otros autores, las muestras analizadas de material piroclástico del volcán Viedma tienen contenidos de 64-66% SiO_2 y que otros aparatos de la ZVA son volcanes esencialmente monolitológicos dacíticos/andesíticos, el edificio del volcán Viedma estaría compuesto principalmente de basaltos o las rocas más antiguas de su basamento tienen un bajo contenido de sílice.

Palabras claves: ASTER, Volcán Viedma, Contenido SiO_2, Zona Volcánica Andina Austral, Chile.

1. Introduction

The Viedma volcano, located at 49°22'S, 73°19'W, is a Holocene active volcano that belongs to the Austral Volcanic Zone (AVZ) (*e.g.*, González-Ferrán, 1995; Stern, 2004). The Viedma volcano is situated northeast of the Viedma Lake, and surrounded by the Viedma glacier in the Southern Patagonian Ice Field. The volcano is 1,500 m high above sea level and exposes only a part of its edifice above the surface of the glacier. Killian (1990) reported that the latest eruption occurred from a subglacial vent in 1988 deposited ash and pumice on the Viedma glacier, and the deposits were re-mobilized and flowed into the Viedma Lake as a lahar. Subsequently, Stern and Killian (1996) reported geochemical data having an adakitic signature and 64-66 wt% SiO_2 contents for the ash and pumice from the Viedma volcano. However, lithological variations that compose the edifice of the Viedma volcano have not been well-documented yet, due to inaccessibility and the prevailing heavy weather conditions.

Aiming to understand the lithological variation over the volcano, we employed the remote sensing techniques. The Advanced Spaceborne Thermal Emission and Reflection radiometer (ASTER) sensor, recently developed by Japanese Ministry of Economy, Trade and Industry (METI), is a powerful tool to map the composition of surface exposures. ASTER has 3 bands (band 1~3) in visible and near infrared range (VNIR) with spatial resolution of 15 m x 15 m, 6 bands (band 4~9) in short wave infrared range (SWIR) with spatial resolution of 30 m x 30 m, and 5 bands (band 10~14) in thermal infrared range (TIR) with spatial resolution of 90 m x 90 m (Table 1). The ASTER sensor, having 11 bands in SWIR and TIR wavelength range, enables highly effective geological mapping, because rocks and minerals have its own inherent spectral pattern in SWIR and TIR range. Using this characteristic, we can classify and detect the type of exposed rocks and mineralization, and estimate the mineral contents quantitatively in some case. In this paper, we used ASTER images covering the overall body of the Viedma volcano to address the variation of SiO_2 contents of the edifice.

2. Estimation of SiO_2 contents

The difference of emission spectrum characteristics caused by the SiO_2 contents is remarkable in the TIR. The absorption of TIR by silicate minerals is correlated to the molecular structure and silica content. For example, mafic minerals have large absorption at band 13 (11.5 μm) and felsic minerals at band 12 (9 μm) (*e.g.*, Conel, 1969; Hunt and Vincent, 1968; Hunt, 1980). Since igneous rocks are classified by the assemblages of silicate minerals and their quantity, the type of igneous rocks and approximate silica content can be indirectly inferred from the TIR absorption position. Figure 1 shows the emission spectrum of various igneous rocks in the TIR.

TABLE 1. BAND-WAVELENGTH-SPATIAL RESOLUTION.

sensor range	ASTER band no.	wavelength (μm)	spatial resolution
VNIR	1	0.520 – 0.600	15 m
	2	0.630 – 0.690	
	3n	0.760 – 0.860	
	3b	0.760 – 0.860	
SWIR	4	1.600 – 1.700	30 m
	5	2.145 – 2.185	
	6	2.185 – 2.225	
	7	2.235 – 2.285	
	8	2.295 – 2.365	
	9	2.360 – 2.430	
TIR	10	8.125 – 8.475	90 m
	11	8.475 – 8.825	
	12	8.925 – 9.275	
	13	10.25 – 10.95	
	14	10.95 – 11.65	

Based on this theory, the rock types and approximate SiO_2 contents of igneous rocks can be estimated using the emissivity ratio (band13/band12). However, this method yields relatively large errors when a target area has high SiO_2 content. To minimize the error, an approach to estimate SiO_2 wt% using ASTER VNIR, SWIR and TIR data was developed by means of multivariate analysis (ERSDAC, 2005). Stepwise regression analysis was used to determine the parameters using SiO_2 wt% as a dependent variable, and the emissivity ratio, bands 1-9, and their ratios such as band2/band1 and band4/band5 as independent variables. The significant independent variables identified by the analysis were band13/band12 and band2/band1. The resulting SiO_2 wt% estimation equa-

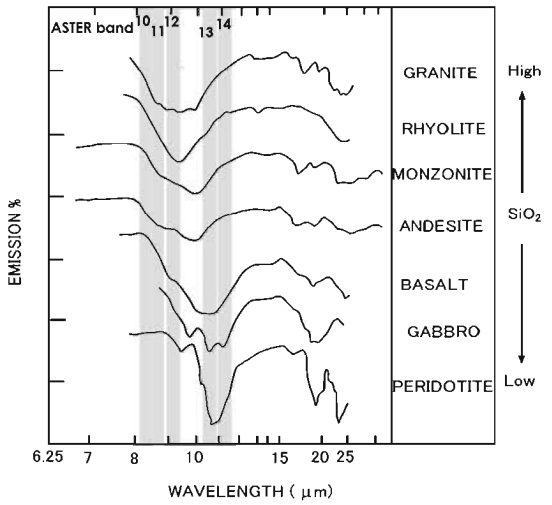

FIG. 1. Spectral characteristics of igneous rocks in thermal infrared region. Vertical gray bands indicate the ranges of five ASTER TIR bands.

tion is given below. The estimation accuracy of the equation is R^2=0.74.

SiO_2 (wt%)=138.42x(band13/band12)+34.61x (band2/band1) - 129.02 (eq. 1)

where band2/band1 is a proxy for the state of oxidation of iron in rock surface and hence a proxy for the weathering intensity.

3. Results

3.1. False color image and Digital Elevation Model (DEM)

We used VNIR data and assigned band 1 for blue, band 2 for red and (3 x band1+band3)/4 for green to produce false color image (Fig. 2). Objects larger than 15 m x 15 m is shown as a dot with specific color. Green color in the figure 1 indicates vegetation, white is snow and glacier, black is water and gray is rock exposures. Because this ASTER data was acquired in summer (January 03, 2005), outcrops of the Viedma volcano emerge more widely. Based on the VNIR observation, the volcanic edifice was divided into bright parts and dark parts (Fig. 2). The boundary of two colors did not correlate with the topographical elements such as elevation, steepness of slopes and obliquity of sun radiation (shadows). The color difference most likely originated from the color of the outcrops.

Stereoscopic image is acquired using nadir-looking and backward-looking telescopes of band 3 (0.76 to 0.86 μm) in the same orbit. We generated Digital Elevation Model (DEM) from the stereoscopic images. We then created a three dimensional image of Viedma volcano by superimposing the DEM data on the false color image (Fig. 3). The 3D image shows that the north side of the edifice is, compared to the south side, rougher due to erosion by the glacier. Several irregular concave structures are preserved in the southern part of the edifice, some are considered to be recent craters. This interpretation agrees with the report of recent occurrence of eruption on the south side of the edifice by González-Ferrán (1995). A N-S trending 5 km-long lineament was observed in the middle of the volcanic body in this image. Several irregular craters were observed to align on the lineament. This alignment of craters corresponds to the observation of González-Ferrán (1995) who showed that four large craters/calderas, between 1.5 and 4 km in diameter, are located along a N-S line. However 3D observation in this study shows that diameter of the craters is 1.5 km at the maximum. Some of the craters/calderas illustrated in González-Ferrán (1995) were not recognized in this study.

3.2. SiO_2 contents

Preprocessing of ASTER data is illustrated in figure 4. First, we applied atmospheric correction to VNIR data to acquire reflectance data, and atmospheric correction and temperature emissivity separation to TIR data to acquire emissivity data. Second, to apply the equation 1 to the rock exposures, we removed areas affected by cloud, vegetation, ice and side moraine from the data. For noise elimination, a conventional method used in the remote sensing analysis was employed as follows. We excluded the vegetation pixels from calculation using the threshold derived from NDVI (vegetation index), *i.e.*, (band3-band2)/(band3+band2) (Tucker, 1979). Pixels consistently having a high value for bands 1-3 in the VNIR and band 4 in the SWIR indicate cloud. Similarly, ice and snow constantly shows high value in the VNIR three bands. By excluding the pixels having high values in these three bands of the VNIR range, cloud, snow and ice pixels were removed. Moraine was eliminated by visual examination based on the

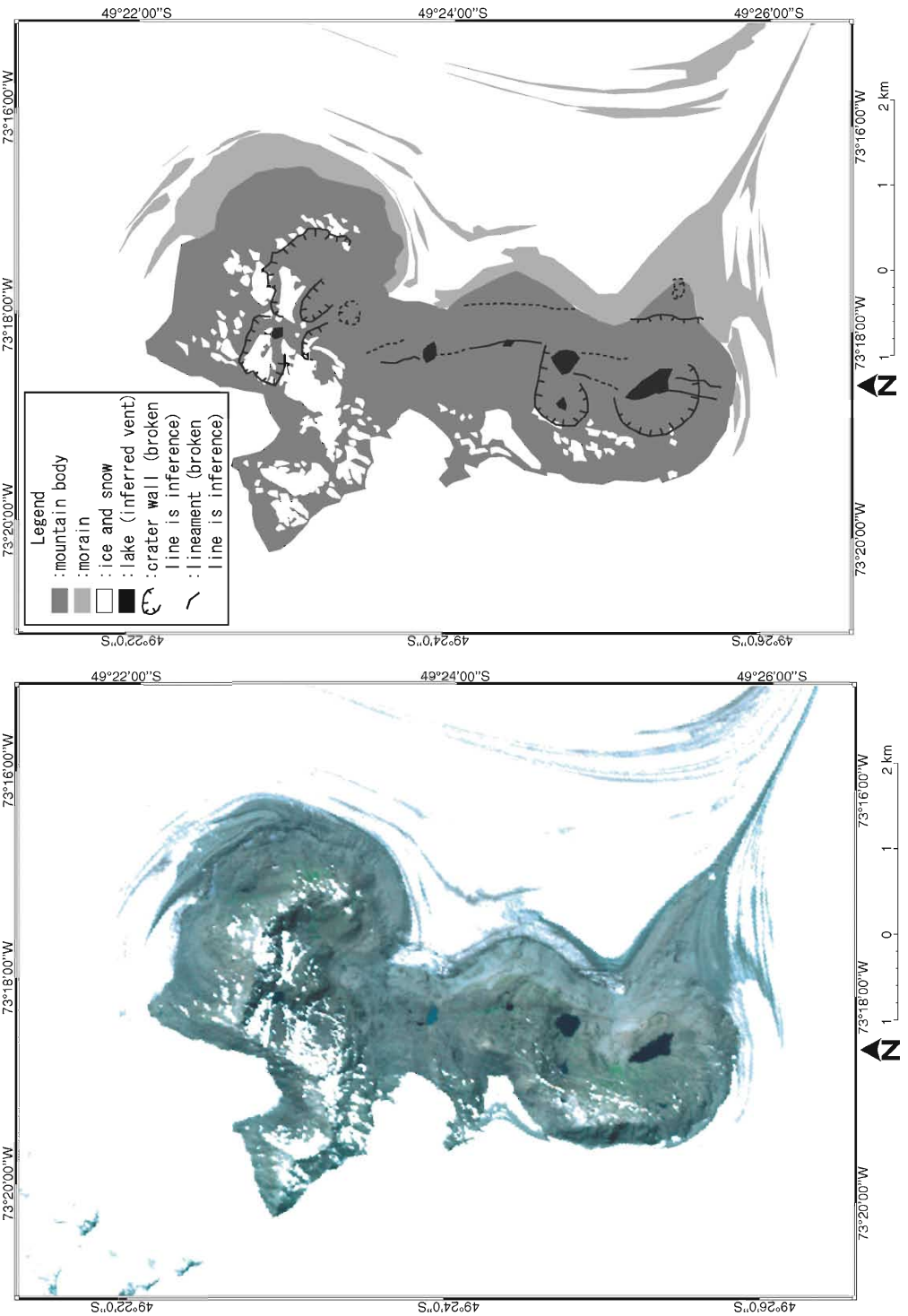

FIG. 2. **Left:** Color composite image of the Viedma volcano generated using data of ASTER VNIR bands acquired on January 03, 2005. **Right:** Landform analysis map of Viedma volcano.

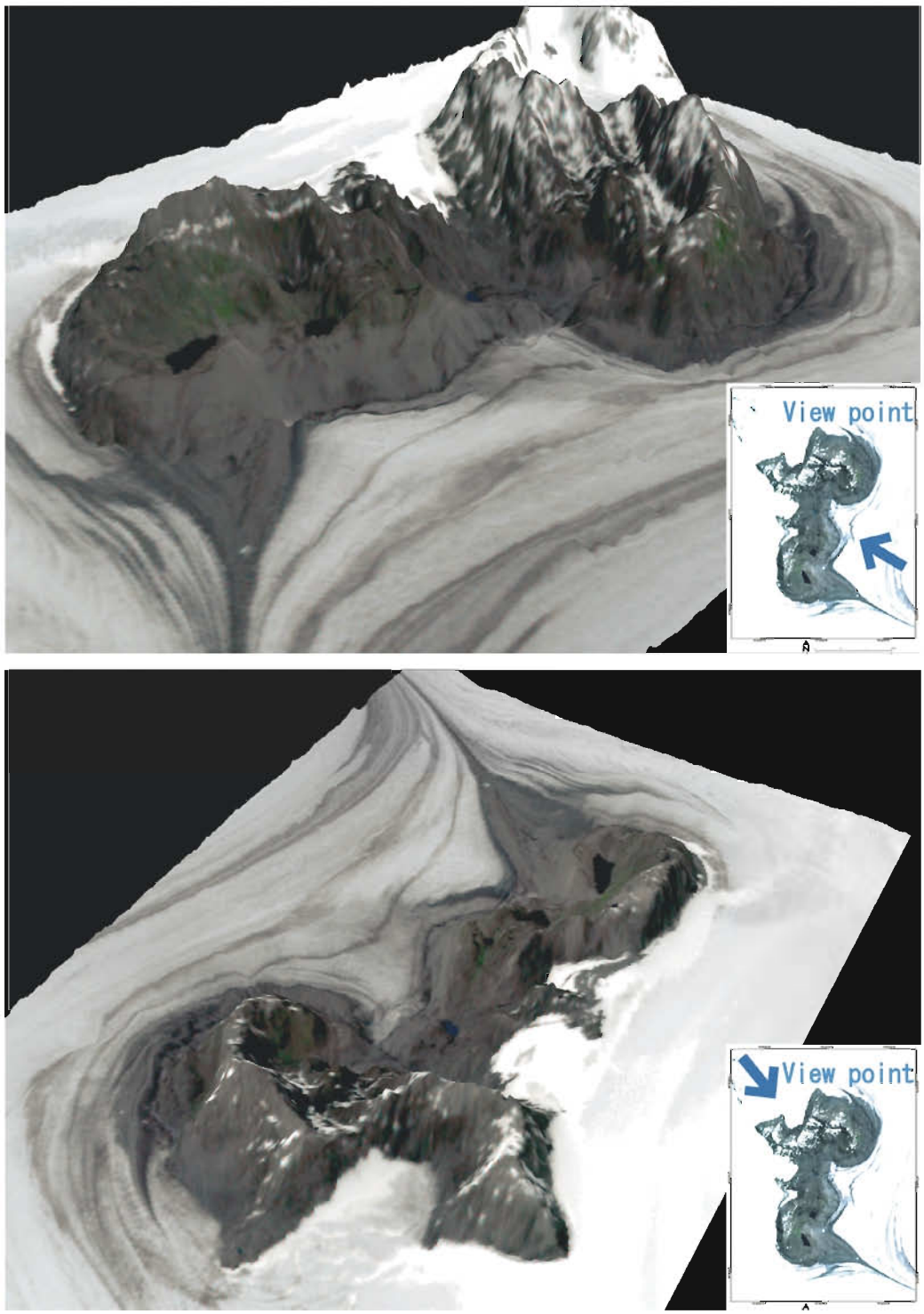

FIG. 3. Bird's eye views. **Upper image:** view from the SE. **Lower image:** view from the NW. These 3D images are produced by overlaying VNIR image on the DEM (Digital Elevation Model). The vertical scale is exaggerated by a factor of 2 to emphasize relief contrasts.

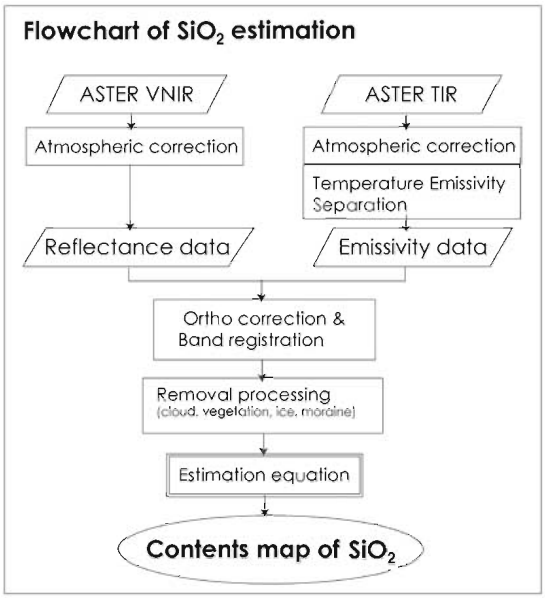

FIG. 4. Flowchart of SiO_2 wt% estimation.

image overlaid on DEM because emissivity of talus slopes such as moraine is known to be different from the original rock as described in ERSDAC (2005).

The result of the SiO_2 estimation is shown in figure 5. Noises were marked in whitish color and water in dark green. Although rock types (igneous, metamorphic or sedimentary) cannot be distinguished, the Viedma volcano has much wider variety of SiO_2 wt% (51-63 wt%), compared to previously published data (64-66 wt% in SiO_2; n=2) (Stern and Killian, 1996). This variation is almost similar to that of the Hudson volcano (50.5-66.6 wt% in SiO_2; Orihashi *et al.*, 2004, 2008), which is one of the largest stratovolcanoes in the southernmost SVZ.

4. Discussion and concluding remarks

The rocks with high SiO_2 contents estimated in this study were distributed at the eastern flank of the edifice and the maximum SiO_2 content was consistent with the reported values (64-66 wt%: *e.g.*, Stern and Killian, 1996). In contrast, we obtained exposures in the central crater area with much lower SiO_2 contents, *i.e.*, basaltic equivalent composition.

In general, talus, regardless if they are basaltic or rhyolitic, tend to exhibit spectral characteristic closer to the rocks with intermediate SiO_2 contents (ERSDAC, 2005). However, patterns of estimated SiO_2 concentration seem to have no strong control of altitude or slope angle, by comparing the pattern in figure 5 to the topographic image in figure 6. Therefore, we infer that the patterns reflect the average SiO_2 concentration of the exposure.

There is a possibility that the Viedma volcano erupted basaltic ejecta or lavas. The Viedma volcano, however, is a small volcano and unlikely to have basaltic or variable compositions that tend to form large volcanic edifice. Furthermore, most other volcanoes in the AVZ are monolithic dacitic/andesite in composition (Stern and Killian, 1996).

Another explanation for the low SiO_2 exposures is distribution of basement rocks having low SiO_2 content. In fact, exposures of Paleozoic metamorphic rocks (metasediments and metabasites) were reported around the Viedma volcano (*e.g.*, Vivallo *et al.*, 1999). Carbonate rock showing no absorption feature around 9 μm was considered to be the potential host rock with low SiO_2 contents, but its diagnostic emissivity absorption near 11.2 μm due to CO_3 vibration was not observed at the Vieldma volcano. Therefore, we conclude that the expected basement exposure is likely metapelites or rocks with basaltic composition (old basaltic edifice or basement of metabasalt).

There are other factors that may lead to underestimation of apparent SiO_2 concentration. At least, two possibilities were assessed before. The first is soil cover on the exposure surface. The second is the influence of hydrothermal alteration, such as sulfide mineralization on the surface. To eliminate such possibilities, validation study that compares the results estimated by ASTER and data sampled at the Viedma volcano will be required in the future.

We demonstrated that the remote sensing technique based on ASTER data is useful tool for reconnaissance and lithological mapping of a volcano as well as semi-quantitative estimation of SiO_2 wt%. In this study, we estimated the SiO_2 wt% of Viedma volcano to vary from 51% to 63%. Although there are some possibilities for lower SiO_2 value (*e.g.*, metamorphic rocks).

Acknowledgements

We are grateful to Dr. Y. Arakawa of Kangean Energy Indonesia Ltd. and colleagues of the CHRISTMASSY (Chile Ridge Subduction to Magma Supply System) Project Group for discussions and supports. We should like to

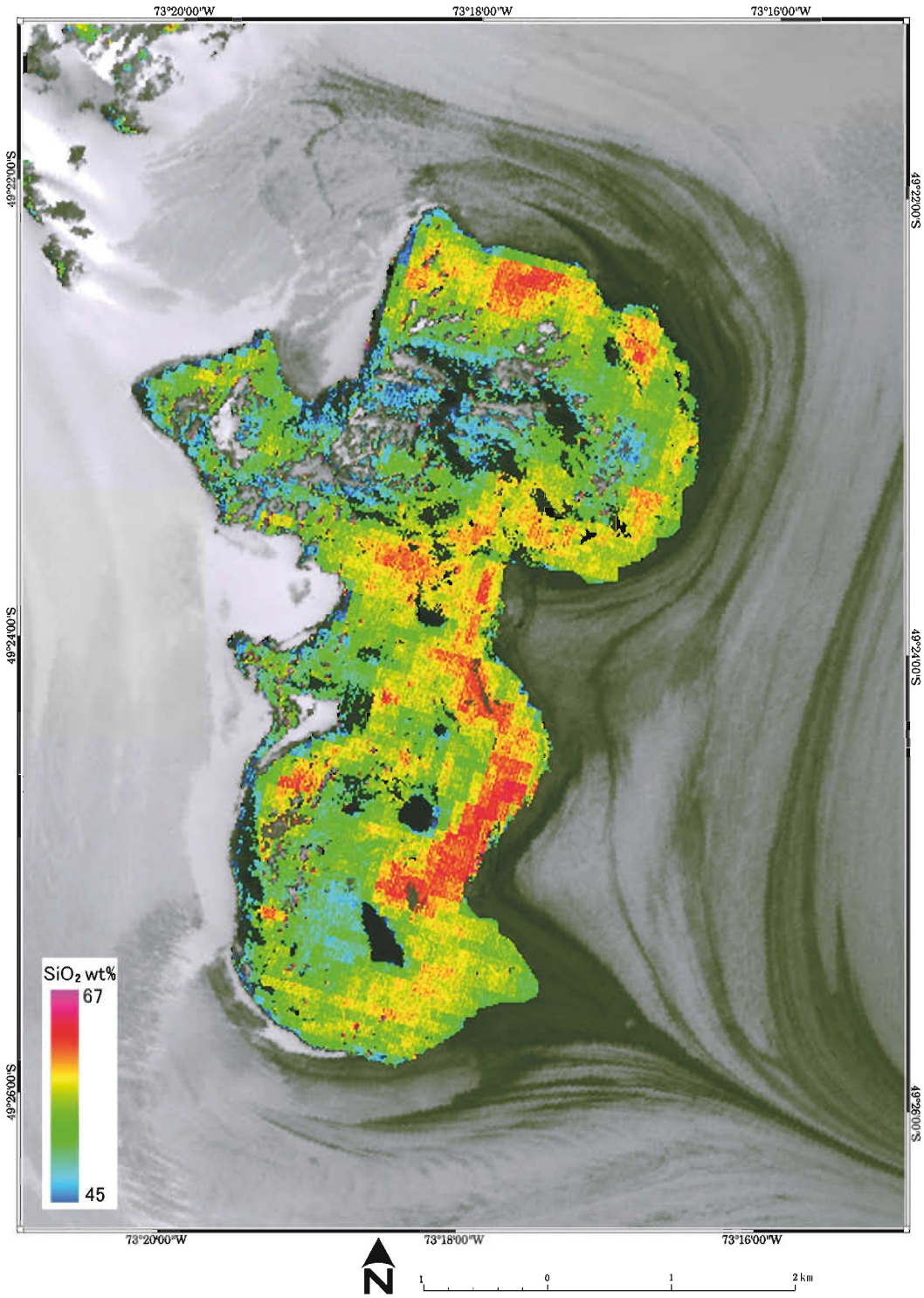

FIG. 5. Map of SiO_2 contents. Viedma volcano has wide variety of SiO_2 contents from 45 wt% to 67 wt%. Typical average SiO_2 content is 51 wt%-63 wt% in most area.

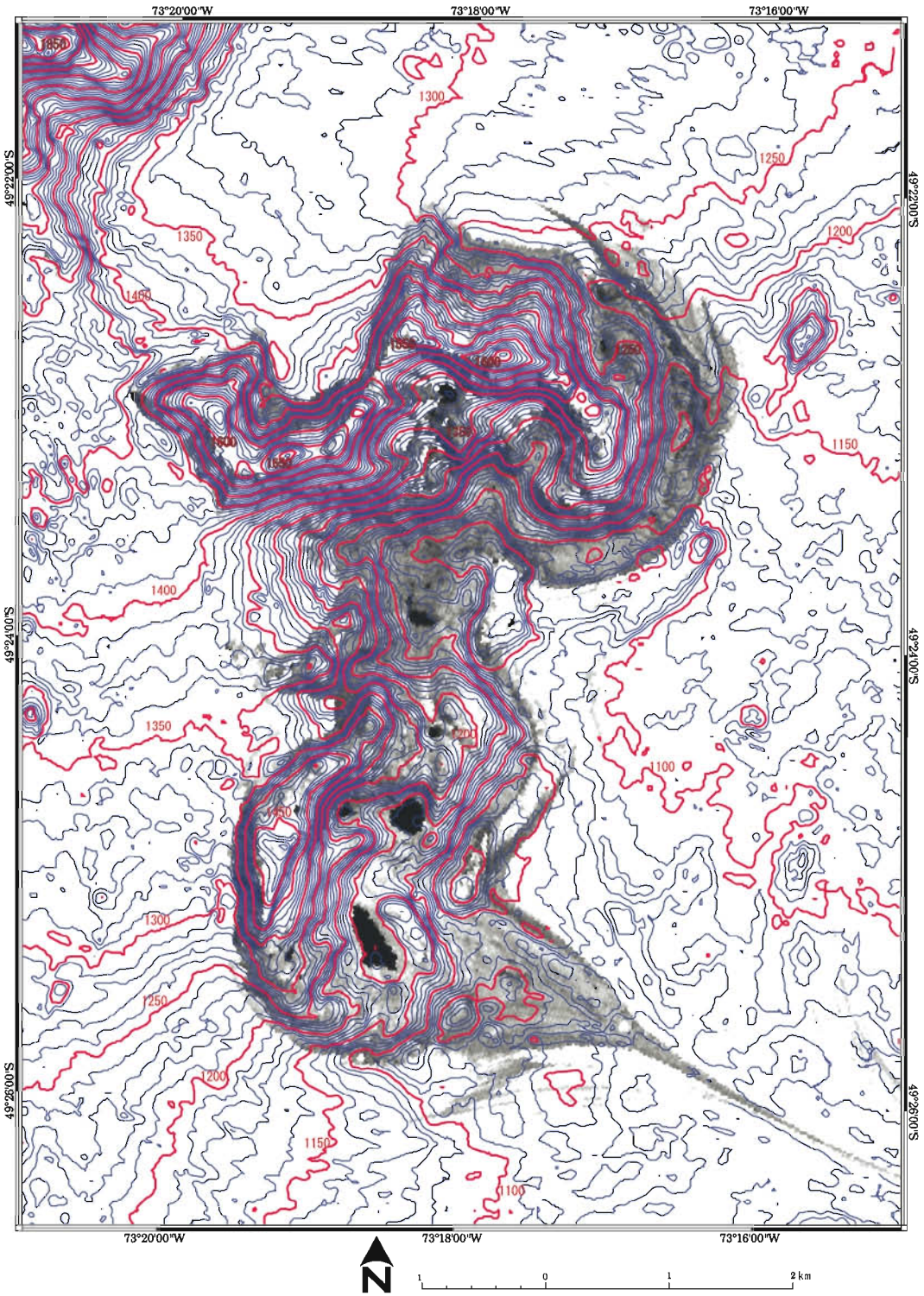

FIG. 6. Contour map. This map is produced by relative ASTER DEM. Red and violet contours are at 50 m and 10 m intervals, respectively.

express our appreciation to Dr. C. Stern, Dr. A. Demant and the anonymous referee for their helpful comments. This research was partly supported by the Earthquake Research Institute of the University of Tokyo cooperative research program (to D.H.).

References

Conel, J.E. 1969. Infrared emissivities of silicates: Experimental results and cloudy atmosphere model of spectra emission from condensed particulate mediums. Journal of Geophysical Research 74 (B6): 1614-1634.

ERSDAC. 2005. Remote sensing application for development of extracting method of high potential resource area from ASTER TIR data, Report on Research and Development of Remote Sensing Technology for Non-renewable Resources (3/4): 171-187. Tokyo, Japan.

González-Ferrán, O. 1995. Volcanoes de Chile. Instituto Geográfico Militar: 640 p. Santiago.

Hunt, G.R. 1980. Electromagnetic Radiation: The Communication Link in Remote Sensing. *In* Remote Sensing in Geology (Siegal, B.S.; Gillespie, A.R.; editors). John Wiley: 5-45. New York.

Hunt, G.R.; Vincent, R.K. 1968. The behavior of spectral features in the infrared emission from particulate surface of various grain size. Journal of Geophysical Research 73 (B18): 6039-6046.

Killian, R. 1990. The Austral Andean Volcanic Zone (South Patagonia). *In* International Symposium on Andean Geology (ISAG), No. 1, Abstract: 301-305. Grenoble, France.

Orihashi, Y.; Nakai, S.; Shinjoe, H.; Naranjo, J.A.; Motoki, A.; CHRISTMASSY Group 2008. Magmatic evolution of the Quaternary volcanics from Hudson and Lautaro volcanoes, Austral Andean Cordillera. *In* Goldschmidt Conference, No.18, Geochimica et Cosmochimica Acta Special Supplement 72 (12): p. A709. Vancouver, Canada.

Orihashi, Y.; Naranjo, J.A.; Motoki, A.; Sumino, H.; Hirata, D.; Anma, R.; Nagao, K. 2004. Quaternary volcanic activity of Hudson and Lautaro volcanoes, Chilean Patagonia: new constraints from K-Ar ages. Revista Geológica de Chile 31 (2): 207-224.

Stern, C. 2004. Active Adean volcanism: its geologic and tectonic setting. Revista Geológica de Chile 31 (2): 161-206.

Stern, C.; Killian, R. 1996. Role of the subducted slab, mantle wedge and continental crust in the generation of adakite from the Andean Austral Volcanic Zone. Contributions to Mineralogy and Petrology 123: 263-281.

Tucker, C.J. 1979. Red and photographic infrared linear combinations for monitoring vegetation. Remote Sensing of Environment 8: 127-150.

Vivallo, W.; Gardeweg, M.; Tassara, A.; Zanettini, J.; Márquez, M.; González, R. 1999. Mapa de recursos minerales del área fronteriza Argentino-Chilena entre los 34° y 56°S. Servicio Nacional de Geología y Minería y Servicio Geológico Minero Argentino. Publicación Geológica Multinacional No. 1, escala 1:1.000.000.

Manuscript received: July 29, 2009; revised/accepted: April 19, 2010.